

The molecular basis of TnrA control by glutamine synthetase in *Bacillus subtilis*

Ksenia Hauf¹, Airat Kayumov², Felix Gloge³, Karl Forchhammer¹

¹ Interfaculty Institute for Microbiology and Infection Medicine, University of Tuebingen, Auf der Morgenstelle 28, 72076 Tuebingen, Germany

² Kazan Federal University, Department of Genetics, Kremlevskaya 18, 420008, Kazan, Russia

³ Wyatt Technology Europe Hochstrasse 12a, 56307 Dernbach, Germany

Running title: Molecular basis of TnrA control by glutamine synthetase

To whom correspondence should be addressed: K. Forchhammer, Interfaculty Institute of Microbiology and Infection Medicine, University of Tuebingen, Auf der Morgenstelle 28, D-72076 Tuebingen, Germany, Tel: +49 70712972096, Fax: +49 7071295843
E-mail: karl.forchhammer@uni-tuebingen.de

Keywords: transcription factor TnrA, glutamine synthetase, transcription regulation, AMP, glutamine, glutamate, ATP, *Bacillus subtilis*

ABSTRACT

TnrA is a master regulator of nitrogen assimilation in *Bacillus subtilis*. This study focuses on the mechanism of how glutamine synthetase (GS) inhibits TnrA function in response to key metabolites ATP, AMP, glutamine and glutamate. We suggest a model of two mutually exclusive GS conformations governing the interaction with TnrA. In the ATP-bound state (A-state), GS is catalytically active, but unable to interact with TnrA. This conformation was stabilized by phosphorylated MSX, fixing the enzyme in the transition state. When occupied by glutamine (or its analogue MSX), GS resides in a conformation that has high affinity for TnrA (Q-state). The A- and Q-state are mutually exclusive and in agreement, ATP and glutamine bind to GS in a competitive manner. At elevated concentrations of glutamine, ATP is no more able to bind GS and to bring it into the A-state. AMP efficiently competes with ATP and prevents formation of the A-state, thereby favoring GS-TnrA interaction. SPR analysis shows that TnrA bound to a positively regulated promoter fragment binds GS in the Q-state whereas it rapidly dissociates from a negatively regulated promoter fragment. These data imply that GS controls TnrA activity at positively controlled promoters by shielding the transcription factor in the DNA-bound state. According to size-exclusion and multi-angle light scattering analysis (MALS), the dodecameric GS can bind three TnrA dimers. The highly interdependent ligand binding properties of GS reveal this enzyme as a sophisticated sensor of the nitrogen and energy

state of the cell to control the activity of DNA-bound TnrA.

INTRODUCTION

The Gram-positive soil bacterium *Bacillus subtilis* is able to utilize nitrate, nitrite and urea in the absence of its preferred nitrogen sources like ammonium ions or glutamine (1-3). The metabolism of such compounds tightly regulated and requires a large energy investment. Under conditions of nitrogen limitation, the global transcription regulator TnrA activates genes and operons of nitrate and nitrite reduction (*nasABCDEF*), urea (*ureABC*) and nucleotide assimilation, ammonia transport (*nrgAB*) and its own gene. Meanwhile it represses operons required for ammonium assimilation like the *glnRA* and *gltAB* operons (1,4-6). Furthermore, TnrA was suggested to be involved in the control of amino acid and purine utilization and might even be involved in oxidative stress response (7).

Under nitrogen-poor conditions, TnrA interacts with the P_{II}-like protein GlnK, which itself is membrane-associated via the ammonium transporter AmtB (3,8). After sudden exposure to nitrogen-excess conditions, TnrA is released from GlnK (8) and its transcriptional activity is repressed by interaction with GS. Previous biochemical studies demonstrated that GS can only interact with TnrA in the presence of GS feedback-inhibitors glutamine or AMP and this interaction would prevent DNA-binding activity of TnrA (9). Furthermore, feedback-inhibited GS stabilizes

DNA-binding activity of GlnR, a repressor for *glnRA* and *ureABC* operons as well as the *tnrA* gene (10). Therefore, GS in *Bacillus subtilis* is regarded as a trigger enzyme, which participates in primary metabolism and controls gene expression indirectly through TnrA and GlnR (9,11,12).

Both transcription factors (TnrA and GlnR) have a high sequence similarity at the N-terminus and bind the same DNA consensus sequence (TGTNAN₇TNACA), in which only 4 nucleotides in each operator half-site are required for their specific DNA-binding (1,5,6,13,14). Three conserved residues of the second α -helix (Tyr32, Arg28, Arg31 of TnrA and Tyr30, Arg26 and Arg29 of GlnR) recognize the consensus sequence (14). TnrA serves in most cases as an activator, whereas in a few cases it acts like GlnR as a repressor (1,5,6). The C-terminus of these proteins differs completely and is considered to be a signal transduction domain (10,14-17). The last 15 C-terminal residues of TnrA interact with GS while GlnK binding occurs in region 75-90 of the C-terminus (9,17). TnrA dimerization is mediated by residues 6-11 in its first N-terminal α -helix and by residues 52-67 of a hydrophobic winged-helix-turn-helix motif (14). In contrast, GlnR requires the feedback-inhibited GS for dimerization and subsequent DNA binding (14,16).

The GS of *B. subtilis* catalyzes the ATP-dependent amidation of glutamate to glutamine in the presence of ammonium. The biosynthesis of glutamine involves the initial phosphorylation of the γ -carboxyl group of glutamate by ATP, followed by ammonium incorporation and release of inorganic phosphate yielding glutamine (18,19). The enzyme forms a dodecamer, which consists of two face-to-face hexameric rings (20). The active sites are located at the interface between neighboring subunits. For each active site, the major part is made up by the C-terminus of one subunit, together with a short segment from the N-terminal domain of the laterally adjacent subunit. During formation of the transition state, a loop region contributed by the N-terminal domain undergoes a major structural rearrangement (20). This catalytically induced structural change leads to significant alterations in the overall dodecamer structure of GS (20).

The activity of GS in *Bacillus subtilis* is tightly regulated via feedback-inhibition by glutamine and AMP (21). The recently published crystal structure also reveals the mechanism for

feedback inhibition by glutamine (20). A central role in glutamine binding is played by an arginine residue from the N-terminal segment (Arg62), which forms hydrogen-bonds with glutamine. This hydrogen bonding network, prevents glutamine release and locks the catalytic center in a closed state, thereby preventing substrate binding and inhibiting catalytic activity.

In addition, the biosynthetic activity of GS is tuned down by the interaction with the transcription factor TnrA, while GlnR does not affect the activity of GS (22). Whereas the GlnR-GS structure is unknown, a crystal structure between GS and a peptide corresponding to the last 36 amino acids of TnrA detected the putative TnrA binding sites in the intersubunit catalytic pores of GS mostly near the catalytic centers (14). However, the complex assembled as a tetradecamer and the physiological relevance of this structure remains elusive.

So far, it is assumed that only feedback-inhibited GS binds to TnrA thereby abolishing the DNA-binding activity of TnrA (9,14). In the present study, we demonstrate that in the presence of glutamine, GS binds TnrA directly on the DNA, forming a ternary GS-TnrA-DNA complex. Through antagonistic interactions between the effector molecules, TnrA-GS complex formation is regulated by the intracellular levels of ATP, AMP, glutamine and glutamate. Therefore, it seems that GS has a so far underestimated role as sophisticated sensor of the cellular nitrogen- and energy state.

EXPERIMENTAL PROCEDURES

Strains and plasmids

Bacillus subtilis strains and plasmids used in this study are presented in Table 1. To obtain the plasmid pDG-TnrA-ST, the *tnrA* gene was amplified from *B. subtilis* genomic DNA using primers *tnrA* for (AAA GTC GAC ATG ACC ACA GAA GAT CAT TCT TAT) and *tnrA* rev (AAA AAG CTT TCA TTA ACG GTT TTT GTA CCG AAA GTG). The PCR product was digested with SalI and HindIII, and cloned into the expression vector pGP380 (23) cut with the same enzymes to obtain plasmid pGP380-TnrA. Further, the *tnrA* gene containing N-terminal StrepII-tag was amplified by PCR using plasmid pGP380-TnrA and primers *tnrA* ST for (T AAC AAG CTT AAT ACC TAG GAC TCG TTC AC) and *tnrA* rev. The PCR product was cloned into the HindIII site of the expression vector pDG148.

To obtain the StrepII-tagged *tnrA* gene under the control of its own promoter, the promoter region of *tnrA* was amplified using *B. subtilis* genomic DNA and primers ptnrA for (TC TTC GAA TTC GAT TAT CCT TCC TCC TCG) and ptnrA rev (TT TTC CCC GGG TGG ATG TCT TTT GAT AAT AG). The plasmid pGP380-TnrA was digested with EcoRI and SmaI to remove the constitutive degQ36 promoter, and ligated with the PCR product containing the promoter region of *tnrA*.

The *glnA* gene was amplified from the genomic DNA *B. subtilis* using primers glnA for (CATCA TCATC ATCAT CACAG CAGCG GCCTG GTGCC GCGCG GCAGC CATAT GGCAA AGTAC ACTAG AGAAG) and glnA rev (GCTCA GCGGT GGCAG CAGCC AACTC AGCTT CCTTT CGGGC TTTGT TATTA ATACT GAGAC ATATA CTGTTC). The pET15b plasmid was digested with the restriction endonuclease BamHI. The PCR product and the digested plasmid were assembled using an isothermal, single-reaction method for assembling multiple overlapping DNA molecules as described previously (24).

Plasmid pGP177 was generated for overexpression of the N-terminally StrepII-tagged GS in *B. subtilis*. The *glnA* gene was amplified from plasmid pGP174 using the primer pairs CD23/CD24 (AAAGG ATCCG AATGA CAAAG GAGCT GAGGA TCATG GCTAG CTGGA GCCAC CCGCAG/ AAAAT GCATT CATT AACTG ATACT GAGAC ATATA CTGTTC). The PCR product was digested with BamHI and NsiI, and ligated with plasmid pBQ200 that was cut with BamHI and PstI. The sequence integrity of all genes was confirmed by DNA sequencing.

B. subtilis cells were grown in Spizizen minimal medium (SMM) (25) containing glucose (0.5% (w/v)) as a carbon source. As a nitrogen source 20 mM sodium nitrate, 1.5 or 15 mM glutamine was used. L-tryptophan was added to a final concentration of 50 mg per liter. For recombinant strains, kanamycin, erythromycin or chloramphenicol were added until final concentration of 10 mg per liter.

In vivo crosslinking and SPINE assays

The *in vivo* cross-linking of proteins was performed as described in (23). *B. subtilis* recombinant cells producing the StrepII-tagged TnrA, GS or GlnK proteins (*B. subtilis* Δ *tnrA* pGP-*pTnrA*-ST; *B. subtilis* Δ *glnK* pDG-*GlnK*-ST; *B. subtilis* GP251 pGP177) were grown in SMM

supplemented with either 1.5 mM or 15 mM glutamine as indicated. At the late exponential phase of growth ($OD_{600} \sim 0.7$) paraformaldehyde (PFA) was added until a final concentration of 0.6 % (w/v) and incubation was further continued for 20 min. Subsequently, cells were harvested by centrifugation, broken by FastPrep-24 (M.P. Biomedical, Irvine, CA, USA) using 0.1 mm glass beads and the cell-free crude extracts prepared as described previously (17).

StrepII-tagged proteins were purified on Strep-tactin Sepharose as recommended (IBA life sciences). The elution fractions were further analyzed by immunoblotting.

Protein purification

StrepII-tagged GS was overexpressed using pGP174 plasmid (8), StrepII-tagged TnrA was overexpressed using pDG-TnrA-ST plasmid in *E. coli* BL21 (DE3) (Stratagene) and all proteins were purified as described previously (8). His₆-tagged TnrA and GS proteins were overexpressed using pET15b vector and purified as reported previously (22).

Surface Plasmon Resonance Detection (SPR)

SPR experiments were performed using a BIAcore X biosensor system (Biacore AB, Uppsala, Sweden). The biotinylated DNA duplexes were generated as described in (26) and immobilized onto the sensor surface of the streptavidin (SA) sensor chip (Biacore, GE Healthcare), with a flow rate of 10 μ l/min to receive a binding signal of approximately 1500 resonance units (RU). Control DNA duplexes were loaded on flow cell 1 (FC1) and specific DNA duplexes with a TnrA-binding site were loaded on flow cell 2 (FC2). The running buffer used for DNA immobilization contained 10 mM HEPES pH 7.4, 100 mM NaCl, 0.2 mM EDTA and 0.005% Nonidet P-40. Subsequently, purified TnrA was injected to the DNA-loaded SA sensor chip at the concentration of 2.5 μ M (dimer) to receive a binding signal of approximately 2000 RU, which corresponds to a surface concentration change of 2 ng/mm². Subsequently, purified GS at the concentration 0.100 μ M (dodecamer) was loaded on the TnrA-DNA-chip surface with a flow rate 15 μ l/min in the running buffer contained 10 mM HEPES pH 7.4, 300 mM NaCl, 3 mM MgCl₂ x6H₂O, 0.2 mM EDTA and 0.005% Nonidet P-40. For regeneration of the sensor chip surface 2 M NaCl was used.

To test TnrA interaction with different DNA fragments, the indirect capture strategy was used (27). First, a biotinylated single-stranded DNA capture linker (Biotin-gcaggaggacgtaggtagg) was irreversibly bound to a SA chip. Then, a partially double-stranded DNA oligomer that contained the sequence of interest in the double stranded region (Table 2) with a single-stranded overhang complementary to the capture linker, was fixed on the chip as described in (27). The protein of interest was injected as described above. At the end of the experiment, the captured oligonucleotide was stripped from the linker by 1.0 M NaCl, 50 mM NaOH to regenerate the chip.

To immobilize purified TnrA-His₆ on the Ni²⁺-loaded NTA sensor chip, 30 µl of a 2 µM TnrA-His₆ solution (of the dimer) was injected in FC2 until a binding signal of 2000 resonance units (RU) was reached. To measure the binding of GS with TnrA, 100 nM solution of GS-ST (dodecamer) was injected to the TnrA-His₆ surface at 25 °C in HBS-Mg buffer contained 10 mM HEPES pH 7.4, 200 mM NaCl, 3 mM MgCl₂·6H₂O and 0.005% Nonidet P-40, in the presence or absence of ATP, glutamine or MSX.

To test the TnrA:GS stoichiometry, 10 µl of a 5 µM GS-His₆ solution (of the dodecamer) was injected in FC2 the Ni²⁺-loaded NTA sensor chip until a binding signal of 5000 resonance units (RU) was reached. Further, a solution of TnrA-ST with different concentration was injected to the GS-His₆ surface at 25 °C in HBS-Mg buffer contained 10 mM HEPES pH 7.4, 150 mM NaCl, 3 mM MgCl₂·6H₂O, 1 mM glutamine and 0.005% Nonidet P-40. Prior to load fresh TnrA-His₆ or GS-His₆ protein on the NTA sensor chip, bound proteins were first removed by injecting 10 µl of 1 M Imidazol pH 7.0. The stoichiometry between GS and TnrA was calculated using formula (1):

$$R_{max} = \left(\frac{\text{mol. mass analyte}}{\text{mol. mass ligand}} \right) \times \text{response for ligand capture} \times \text{stoichiometry}$$

The resonance difference between FC2 and FC1 (ΔRU) was measured to quantify specific binding to FC2. SPR data were evaluated using the BIAevaluation (Biacore AB) and GraphPad Prism (GraphPad Software, San Diego, California).

Isothermal Titration Calorimetry for Determination of Binding Constants

ITC experiments were performed on a VP-ITC microcalorimeter (MicroCal, LCC) in 10 mM Hepes pH 7.4, 5 mM MgCl₂·6H₂O, 50 mM KCl, 50

mM NaCl at 20°C (17). For determination of ATP, glutamine and AMP binding isotherms for GS, 20 µM or 10 µM protein solution (dodecamer) was titrated with glutamine, ATP or AMP in concentrations ranging from 1.25 mM to 8 mM as indicated. The ligand (6 µl) was injected 45 times into the 1.4285 ml cell with stirring at 155 rpm. The binding isotherms were calculated from received data and fitted to a six-site binding model with the MicroCal ORIGIN software (Northampton, MA).

In vitro cross-linking of proteins

Proteins were dialyzed overnight in a 10 mM potassium phosphate buffer pH 7.4, 100 mM NaCl, 3 mM MgCl₂ and 20% glycerol. The reaction mixture of 1 dodecameric GS and 6 dimeric molecules of TnrA consisted of 1.5 µg/µl of dialyzed GS and 0.45 µg/µl of dialyzed TnrA, mixed in presence of 1 mM Gln, 1 mM MSX and 1 mM ATP as required. The protein mixture was treated with 0.1% freshly prepared solution of glutaraldehyde for 3 minutes at 37 °C. The reaction was stopped by addition of 100 mM Tris pH 7.4.

Size-exclusion chromatography and multi-angle light scattering analysis

Analytical size exclusion chromatography was carried out on an Äkta Purifier System equipped with a Superdex 200 column PC 3.2/30 (GE Healthcare, geometric column volume [V_c] of 2.4 ml) or Superose 6 Increase 3.2/300 (GE Healthcare, geometric column volume [V_c] of 2.4 ml). The cross-linked sample was centrifuged for 5 min at 12 000 rpm and 10 µl of the supernatant were injected for analysis with a flowrate 0.05 ml/min. The running buffer consisted of 10 mM HEPES pH 7.4, 150 mM NaCl, 3 mM MgCl₂ and 0.02% sodium azide. The apparent molecular weights of proteins were estimated after calibration of the column with standard proteins: thyroglobulin (670 kDa), ferritin (440 kDa), globulin (158 kDa), conalbumin (75 kDa), ovalbumin (44 kDa), carbonic anhydrase (29 kDa), RNase (13.7 kDa), aprotinin (6.5 kDa) (Bio-Rad gel filtration standard; GE Healthcare LMW gel filtration calibration kit).

Multi-angle light scattering experiments were carried out with a miniDawn Treos system (Wyatt Technology Corporation) and concentration determination was done with a Optilab rEX refractometer (Wyatt Technology Corporation). The system was connected to a HPLC system with autosampler (Agilent 1260). Samples for analysis were centrifuged for 20 minutes at 12 000 rpm and subsequently filtered through a 20 nm syringe filter

(GE Healthcare) before injection on a Superose 6 10/300 column (GE Healthcare). 50 μ l of the crosslinked sample were loaded with a flowrate of 0.5 ml/min. The column was equilibrated with PBS, pH 7.4, 150 mM NaCl with 0.02% sodium azide to prevent microbial growth. Resulting data was analyzed with ASTRA (Wyatt Technology Corporation). The experiments were carried out at room temperature and the molecular weight was calculated from an average of two injections. The elution volume was plotted against the UV-signal and the molecular weight derived from the light scattering data.

RESULTS

Glutamine synthetase interacts in vivo with TnrA under both nitrogen-rich and nitrogen-limited conditions

It was previously shown that a *B. subtilis* GS-mutant strain constitutively expresses TnrA-dependent genes under nitrogen excess conditions due to the lack of TnrA-inhibition by feedback inhibited GS (1). We raised the question whether GS contributes to TnrA control also under nitrogen-limiting conditions. Therefore, we studied the *in vivo* activity of TnrA in *B. subtilis* reporter strains using a β -galactosidase reporter gene expressed from the TnrA-dependent *nrgA* promoter in a *glnA*⁻ (GP251) and a *glnA*⁺ (GP250) genetic background (3). At a glutamine concentration of 1.5 mM as sole nitrogen source, the activity of β -galactosidase was almost identical to that in nitrate-grown GP250 cells. This indicates that growth with 1.5 mM glutamine results in a similar activation of TnrA than growth with nitrate as sole N-source, considered to be nitrogen-limited (Fig. 1). With 1.5 mM glutamine, the GS-deficient mutant exhibited a 2-fold higher β -galactosidase reporter activity than wild type cells. This derepression in the GS-deficient background indicates that even under conditions of nitrogen limitation, GS partially depresses TnrA activity.

Next, the interaction of TnrA with GlnK and GS under different nitrogen conditions was evaluated using SPINE analysis (23). Therefore, *tnrA*-, *glnK*- and *glnA*-deficient mutants were transformed with plasmids encoding the respective StrepII-tagged proteins (TnrA-ST, GlnK-ST and GS-ST). The recombinant proteins were then extracted with Strep-Tactin Sepharose from extracts of nitrogen-limited cells (1.5 mM glutamine) and cells shifted to nitrogen-rich

conditions (15 mM glutamine) In agreement with previous studies (8,17), GlnK was co-eluted together with TnrA-ST from extracts of nitrogen-limited cells (Fig. 2 A). After shifting the cells to glutamine-rich conditions prior to PFA cross-linking, no GlnK could be detected. However, GS was co-purified with TnrA-ST from both nitrogen-limited cells and cells supplemented with 15 mM glutamine. These observations were confirmed by the reverse SPINE experiments, using GlnK-ST or GS-ST producing strains. TnrA was co-purified with GlnK only from extracts of nitrogen-limited cells (Fig. 2 B), whereas it was bound to GS-ST in both, N-excess and N-limited cells (Fig. 2 B).

Antagonistic effects of effector molecules on GS-TnrA complex formation

The above data suggested that GS interacts with TnrA under both nitrogen-limiting and nitrogen-rich conditions (Figs. 1 and 2), corroborating previous *in vitro* data, showing that feedback inhibitors glutamine and AMP enhance TnrA-GS interaction but are not strictly required (17). Therefore, we wanted to gain deeper insight how GS-TnrA interaction is affected by metabolites and investigated GS-TnrA complex formation by Surface Plasmon Resonance (SPR) spectroscopy. His₆-tagged TnrA was fixed on the surface of a Ni-NTA sensor chip and the StrepII-tagged GS was used as an analyte in the presence of various effectors (Fig. 3). In the absence of any effector molecules, a clear binding of GS to TnrA was observed. The addition of glutamine increased the amount of GS binding to TnrA by about 50%, whereas ATP almost completely abolished TnrA-GS interaction. Interestingly, in the presence of glutamine, ATP could not abrogate TnrA-GS interaction (Fig. 3 A). The calculated association rate (k_{on}) in the presence of glutamine ($k_{on} = 1.75 \times 10^5 \text{ M}^{-1}\text{s}^{-1}$) is very similar to the rate in the absence of any effector molecules ($k_{on} = 1.43 \times 10^5 \text{ M}^{-1}\text{s}^{-1}$). This reveals that not the affinity of GS to TnrA is increased by glutamine, but rather the concentration of productively binding GS molecules.

To elucidate the effect of glutamine on the GS-TnrA-complex formation in more detail, we employed the GS inhibitor L-methionine sulfoximine (MSX). MSX binds to the catalytic center of GS as a glutamate analogue (28) where it gets phosphorylated by ATP. The product, MSX-phosphate (MSX-P), irreversibly fixes the enzyme in the transition state (29). MSX in the absence of

ATP stimulated GS – TnrA interaction to the same extent as glutamine (Fig. 3 B), confirming that the glutamine- and MSX-bound forms of *B. subtilis* GS have similar conformations (30). However, when MSX was combined with ATP to generate the transition state analogue MSX-P, GS binding to TnrA was completely abolished (Fig. 3 B).

These results suggest two relevant conformations of GS for TnrA interaction: (1) a TnrA-binding “Q-state”, promoted by glutamine or by MSX and (2), a non-binding “A-state”, which reflects the catalytic active form of GS in absence of glutamine but loaded with ATP. GS seems to be arrested in the A-state by the transition-state analogue MSX-P.

Co-operative versus antagonistic binding of effector molecules to GS

To characterize the binding of ATP and glutamine to GS and study their interdependence, we performed isothermal titration calorimetry (ITC) (Fig. 4). In presence of 5 mM Mg²⁺ ions, a strong binding of either glutamine or ATP was observed (Fig. 4 A, B). Six binding sites were predicted for both glutamine and ATP (5.6±0.16 and 5.5±0.1, respectively) from the titration data fitting using the “One set of sites” model, which did not provide nevertheless an exact fit to interaction signals, apparently because the cooperativity between binding sites. Further fitting using a binding model of six sequential binding sites gave the best fit for both glutamine and ATP titrations. It resolved binding sites for glutamine with K_D's of 6.9 ± 0.53 μM, 2.7 ± 0.20 μM, 27.7 ± 1.69 μM, 4.4 ± 0.24 μM, 175.7 ± 30.25 μM and 24.9 ± 1.3 μM for sites 1 to 6, respectively. The ITC signals for ATP binding could also only be fitted with a six sequential binding sites model. The corresponding K_D's for sites 1 to 6 were calculated to be 15.2 ± 2.27 μM, 41.3 ± 6.6 μM, 18.2 ± 3.69 μM, 184.4 ± 26.32 μM, 55.2 ± 7.15 μM, 515.5 ± 83.33 μM. These values are consistently higher than those for glutamine, indicating that glutamine binds more tightly than ATP. As illustrated in Fig 5, the sites are apparently sequentially occupied in an alternating order of cooperative and anti-cooperative interactions. In the case of glutamine binding, the order is cooperative - anti-cooperative whereas the inverse order is observed in the case of ATP-binding.

As glutamine prevented the negative effect of ATP on TnrA-GS interaction (Fig. 3), an ITC experiment with 2 mM glutamine was performed in

the presence of 2 mM ATP (Fig. 4 C), which is close to its physiological concentration (31). In the presence of ATP, binding enthalpy for glutamine was strongly decreased when compared with the titration in the absence of ATP (compare Fig. 4 C and Fig. 4 A) and titration curves showed a complex behavior resulting from competitive binding. In a series of GS titrations with various glutamine concentrations in presence of 2 mM ATP, a biphasic curve was observed in each case: In the first injections, the enthalpy increased, until a maximum was reached at a glutamine concentration of 173 ± 34.7 μM, that is close to the half-occupation of the 5th site (and subsequent filling of the 6th site) (Fig. 4 A). Subsequently, the heat change signals decreased again, indicating gradual saturation of GS by glutamine (Fig. 4 C).

The reverse experiments, where GS was titrated with ATP in presence of glutamine were also performed (Fig. 4 D). Here, again a biphasic curve was observed. No signal was detected in the first injections. Apparently, glutamine blocked binding of low concentrations of ATP. After several injections, ATP binding resumed and reached a maximal negative enthalpy at an ATP concentration of 421 ± 31.2 μM, followed by saturation of ATP binding. In this case, the minimum point was close to the affinity of the 6th binding site for ATP – 515.5 ± 83.33 μM (see Fig. 4 B). Together, these results show competition between ATP and glutamine for binding to GS.

Furthermore, the effect of AMP against ATP on GS binding was investigated. First, AMP was titrated to GS in the presence of 2 mM ATP. Again, a complex biphasic curve was observed, with a maximum point at an AMP concentration of 186 ± 14.2 μM (Fig. 4 E). In a reverse experiment, when ATP was titrated to GS in presence of 0.5 mM AMP, binding of ATP could only be observed if added in high concentrations (5 mM). Binding enthalpy was 30-fold lower than in absence of AMP and only a minute amount of ATP could bind to GS (Fig. 4 F), reflecting only a residual interaction, possibly because of strong binding of AMP to GS (20). Therefore, it seems that elevated AMP levels prevent formation of the ATP-bound state of GS (A-state).

GS interacts with DNA-bound TnrA

Since TnrA binds to DNA to promote the transcription of TnrA-regulated genes, we investigated how GS affects TnrA - DNA interaction by SPR spectroscopy. The TnrA-

binding region of the *nrgAB* promoter, which is positively regulated by TnrA and that of the *glnRA* promoter, which is negatively regulated by TnrA (1,6) were used as target DNA sequences. An optimization procedure included DNA-duplexes with different length ranging from 17 bp to 163 bp containing only the TnrA recognition sequence or additional unspecific flanking sequences (data not shown). The best specificity and affinity was observed with a DNA-duplex, which was 30 bp in length for the *nrgAB* promoter (AAAACCATGTCAGGAAATCTTACATGAA AA) and a 54 bp long fragment (GATTTGA TGTTAAGAATCCTTACA TCGTAT TGACACATAATATAACA TCACCTA) for *glnRA* promoter, which contains two TnrA-binding sites.

The length and environment of the TnrA-binding region of the *nrgAB* and *glnRA* promoters turned out to be very important for TnrA binding affinity. TnrA associated strongly with the *nrgAB* promoter fragments, whereas the affinity of TnrA to the *glnRA* promoter fragments was much lower and association was followed by a rapid dissociation, independent of the *glnRA* fragment length (data not shown). Next, the effect of GS on TnrA-DNA binding in the presence of 1 mM glutamine was examined (Fig. 6 A, B). A mixture of TnrA and GS at a ratio of 3 (TnrA dimers) to 1 (GS dodecamer) was injected on either *nrgAB* or *glnRA* promoter regions (Fig. 6 A continuous or dashed lines). Surprisingly, when GS was present in the analyte mixture, TnrA still stably associated with the *nrgAB* fragment (Fig. 6 A). This result contradicts previous data that the TnrA-GS complex cannot bind to DNA (9). Clearly, GS could not prevent the binding of TnrA to the *nrgAB* fragment. However, when a mixture of GS and TnrA was injected on the *glnRA* promoter fragment, the resonance signal was two times lower as compared to TnrA in the absence of GS (Fig. 6 A), indicating that GS partially prevented the binding of TnrA to the *glnRA* promoter fragment.

The following SPR assays were performed with two consecutive injections of proteins (Fig. 6B). First, purified TnrA was injected to the DNA-loaded sensor chip, resulting in stable DNA-TnrA complexes. Subsequently, a second injection was performed with purified GS (Fig. 6 B). Surprisingly, when TnrA was already bound to the *nrgAB* promoter, GS could easily form a complex with DNA-bound TnrA in presence of 1 mM

glutamine (Fig. 6 B continuous line). This complex was stable as long as 1 mM glutamine was present in the buffer and quickly dissociated when glutamine was absent (data not shown). However, when TnrA was bound to the *glnRA* promoter fragment, GS could not stably bind, but instead, dissociation of TnrA from the DNA fragment was observed (Fig. 6 B dashed line).

Next, the effect of metabolites on the formation of a *nrgAB* DNA-TnrA-GS complex was tested (Fig. 6 C, D). In the absence of any effectors, a low level of GS binding to DNA-bound TnrA was observed. The presence of 1 mM glutamine resulted in a 5-fold increase of binding (Fig. 6 C - continuous and dashed lines). ATP completely abrogated the binding of GS to the TnrA-DNA complex; however, glutamine prevented the negative effect of ATP on DNA-TnrA-GS complex formation, as observed previously in the TnrA-GS interaction assay (compare Fig. 3 and Fig. 6 C). MSX stimulated GS binding to TnrA in the same way as glutamine (Fig. 6 D - dashed line curve). However, in presence of MSX and ATP, GS could not bind to DNA-associated TnrA.

The influence of different nucleotides on GS interaction with DNA-bound TnrA

The same type of interaction assay was now performed to study the effect of adenyl nucleotides on the binding of GS to DNA-bound TnrA (Fig. 7). Compared to the absence of effector molecules, AMP increased the quantity of GS binding to the DNA-TnrA complex two-fold, which is a much weaker stimulation of binding than that caused by glutamine or MSX (Fig. 7 A). In the presence of AMP and MSX, the resonance signal was the same as in presence of MSX alone (Fig. 7 A). ADP prevented the binding of GS to TnrA to the same extent as ATP (Fig. 7 A). However, in combination with MSX, ADP could not prevent the interaction between GS and DNA-bound TnrA, whereas ATP with MSX again led to a complete loss of binding activity. This confirms that the ATP-dependent phosphorylation of MSX is responsible for the abrogation of GS binding to TnrA (Fig. 7 A). To further corroborate this hypothesis, we tested the effect of non-hydrolyzable analogues of ATP. AMP-PNP was as efficient as ATP in preventing GS-binding to TnrA, indicating that hydrolysis of ATP is not necessary to shift GS into the A-state conformation. However, AMP-PNP could not counteract the binding of MSX-activated GS to TnrA, which agrees with its inability to

phosphorylate GS-bound MSX (Fig. 7 B), The response to ATP γ S, a poorly-hydrolyzable analog of ATP, was also investigated and an intermediary effect between ATP and AMP-PNP was expected. Indeed, in the presence of ATP γ S and MSX, slow binding of GS to the TnrA-DNA surface was observed (Fig. 7 B). Apparently, ATP γ S slowly phosphorylates MSX, with the remaining non-phosphorylated MSX promoting complex formation between GS and TnrA. These experiments clearly establish that phosphorylation of MSX is required to shift GS into the A-state that does not bind TnrA.

The affinity of GS towards TnrA depends on the ratio between feedback-inhibitors and substrate molecules

We next addressed the question, how different ratios of GS substrates and effector molecules affect GS interaction with TnrA. First, the effect of various glutamine concentrations and AMP on the binding ability of GS to DNA-bound TnrA was investigated. A titration was performed with increasing concentrations of glutamine in presence of ATP and glutamate and the steady-state binding of GS was plotted against the glutamine concentration (Fig. 8). In absence of any metabolites, 22 μ M glutamine resulted in half-maximal binding (EC_{50}) of GS to the TnrA-DNA surface (Fig. 8 A). In presence of 1 mM ATP, the EC_{50} for glutamine increased to 90 μ M (Fig. 8 C). To mimic the *in vivo* situation, we tested the effect of glutamine on GS-TnrA interaction in presence of both 1 mM of ATP and 10 mM of glutamate (Fig. 8 E) (31,32). While glutamate alone was not inhibitory for GS-TnrA interaction (not shown), in presence of ATP and glutamate the EC_{50} for glutamine increased to 120 μ M.

The influence of AMP on the interaction of GS with DNA-bound TnrA was also tested (Fig. 8 B, D, F). The steady-state level of GS-TnrA interaction promoted by AMP was about 3-4 times lower than glutamine-promoted GS interaction with TnrA. Moreover, the complex was less stable than in the presence of glutamine and the binding signal decreased following the injection phase. In the absence of other metabolites, the EC_{50} for AMP was 21 μ M. Importantly, AMP could relieve the negative effect of ATP with an EC_{50} of 45 μ M AMP (Fig. 8 D), indicating that already micromolar concentrations of AMP can prevent the formation of the A-state of GS. Surprisingly, in presence of 10 mM glutamate and 1 mM ATP (Fig. 8 F), the

protective effect of AMP on GS-TnrA interaction was more pronounced than with ATP alone (Fig. 8 D) with the EC_{50} for AMP decreasing from 45 μ M to 30 μ M. This result is in perfect agreement with the ITC experiments above (Fig. 4 F), showing that AMP quenches the binding of ATP to GS, and therefore, prevents formation of the A-state.

The stoichiometry of TnrA-GS complex formation

The crystal structure of the TnrA C-terminal peptide in complex with GS was described as a tetradecameric structure of GS with two non-interacting 36 amino acid peptides in each inter-subunit cavity of GS, where the catalytic site is located (14). To study the stoichiometry between full length TnrA and GS, size exclusion chromatography on analytical columns was performed. Using an analytical Superose Increase 6 column, no GS-TnrA complex could be eluted, even in presence of 10 mM glutamine after overnight incubation of the proteins (data not shown). This indicates that the GS-TnrA complex is not stable enough to withstand gel-filtration and dissociates during chromatography. For this reason, proteins were cross-linked with glutardialdehyde to stabilize the complexes. With this method, pure GS in the absence of interaction partners eluted in three peaks with apparent masses of 588 kDa (corresponding to dodecameric GS with 612 kDa), 125 kDa (corresponding to dimeric GS 102 kDa) and 62 kDa (corresponding to monomeric GS with 51 kDa) (Fig. 9 A). Pure TnrA eluted as one peak with an apparent size of 42 kDa (corresponding to dimeric TnrA with 30 kDa). To assay the GS-TnrA complex, a mixture at a ratio of 6 TnrA dimers to one GS dodecamer was set up and supplemented with 1 mM MSX to maximize complex formation. After cross-linking, a peak corresponding to an apparent mass of 649 kDa, was obtained. This elution shift corresponds to a size difference of 61 kDa, which equals two dimeric molecules of TnrA. A comparable size shift of approximately 60 kDa was also observed when the experiment was performed in the presence of glutamine (Fig. 9 B). As a control, we tested the oligomeric state of the TnrA-GS complex in presence of MSX-P to inhibit TnrA-GS interaction. As expected, no shift of the dodecameric GS peak as compared to GS without effectors was observed (Fig. 9 A). These data suggest that at least two dimers of TnrA associate to the dodecameric GS complex. It should be noted that after crosslinking the elution peak tails towards

lower masses, indicating that a heterogeneous population of GS with TnrA and dodecameric pure GS is eluting. Therefore, the size shift underestimates the size of fully TnrA-occupied GS.

To obtain more precise data about the size of the crosslinked complexes we additionally carried out size exclusion chromatography coupled to multi angle light scattering (SEC-MALS). The calculated molar mass of the peak that correspond to dodecameric GS is 684 ± 12 kDa (Fig. 9 C dashed line). The calculated molecular weight of GS-TnrA complex was 787 ± 3.5 kDa (Fig. 9 C straight line). This corresponds to a molecular weight difference of 100 kDa suggesting that three TnrA dimers bind with dodecameric GS. The increase of molecular weight in relation to the theoretical size of the complex is most likely a consequence of glutaraldehyde reacting with surface exposed lysine residues and therefore decorating the complex.

To specify this result, TnrA – GS interaction assays were performed in a quantitative manner by SPR spectroscopy (Table 3). His₆-tagged GS (629 400 Da) was fixed on the surface of a Ni-NTA sensor chip and StrepII-tagged TnrA (29 800 Da) in various concentrations was used as an analyte in the presence of 1 mM glutamine. Saturation of GS by TnrA was only reached at a concentration exceeding 2 μ M TnrA (Table 3). From the ratio between the resonance units (RUs) of surface-bound GS to the maximal RUs after TnrA injection, the stoichiometry was calculated. The results approximates that three TnrA dimers bind to one dodecameric GS molecule (Table 3), which is in good agreement with the gel-filtration and light scattering analysis of cross-linked proteins.

DISCUSSION

Being a trigger enzyme, GS in *B. subtilis* regulates the activity of transcription factor TnrA (1,9) as well as being a central enzyme of nitrogen assimilation. Though considerable advances have been made, many details of the dual role of GS are not yet understood. This study reveals a stunning complexity of the interaction of GS with the effector molecules ATP, AMP glutamine and glutamate and with TnrA. In agreement with the available structural information (20) GS seems to adopt two mutually exclusive conformations: in the presence of ATP, the enzyme is catalytically competent (18,19), but unable to interact with

TnrA. In the presence of glutamine, activity of the enzyme is inhibited (21) but affinity towards TnrA is maximal. In the absence of any effector molecules, GS can interact with TnrA, although quantitatively less binding was observed as compared to GS in the glutamine state. According to the kinetic constants, this difference is due to a lower concentration of productively binding GS molecules. These data agree with a model according to which GS in the absence of effectors resides in an equilibrium between A- and Q-state. Addition of ATP or glutamine shifts this equilibrium either to the A- or Q-state in a concentration-dependent manner. When both effectors are present simultaneously, the equilibrium position depends on the relative concentrations of these metabolites (discussed in more detail below).

In the Q-state, dodecameric GS can bind up to three TnrA dimers according to our SEC and MALS analysis. This result contradicts a recently published work, suggesting a major rearrangement of the oligomeric structure of GS upon binding of TnrA (14) into a tetradecameric complex. SEC and MALS analysis in solution clearly preclude a tetradecameric structure. SPR analysis of GS-TnrA interaction provides an additional strong argument in favor of the formation of GS-TnrA complexes in the dodecameric state: Dodecameric His-tagged GS was immobilized on the Ni-NTA surface of the sensor chip, thereby fixing the structure in an irreversible manner, precluding the interconversion of a GS dodecamer into a tetradecamer. Nevertheless, TnrA bound perfectly to the dodecameric immobilized GS. The tetradecameric structure of GS co-crystallized with the C-terminal peptide of TnrA might be caused by the particular crystallographic conditions. Nonetheless, this structure shows that the interface between opposing subunits of the double hexameric ring constitutes the binding site for the TnrA C-terminus. This corresponds to 6 possible binding sites surrounding the dodecamer. However, we detected only up to three TnrA dimers binding to dodecameric GS, implying that every second site should be occupied by TnrA according to symmetry considerations. The model of three TnrA dimers binding to dodecameric GS corresponds to a previously published non denaturing PAGE analysis of GS-TnrA complexes, where three additional protein bands of higher mass were clearly resolved after adding TnrA to GS (9).

The crystal structure of *B. subtilis* GS revealed that the active sites are located at the interface between two laterally adjacent subunits. Since the enzyme is made up of two face-to-face hexameric rings, each half-enzyme contains 6 active sites (20,33,34). Interestingly, ITC data of GS titration with glutamine or ATP predicted 6 sites in each case instead of the expected 12 sites. In accord, a model of six binding sites gave the best fit of the binding data (Fig. 4). The ITC data evaluation revealed a remarkable pattern of alternating positive (synergistic) and negative (antagonistic) cooperative interactions between the metabolite binding sites of GS (Fig. 5). This indicates a high degree of cooperativity between the subunits. This pronounced intramolecular communication between binding sites could be intimately linked to the sensory properties of this trigger enzyme.

The concept of the two mutually exclusive A- and Q-states of GS, as derived from binding of TnrA is fully supported by the ITC metabolite binding experiments. It also agrees with the crystal structure of GS (20), which showed that the same binding site cannot be occupied by both ATP and glutamine simultaneously. Both effectors were able to displace one another from the active site with glutamine binding being more efficient than ATP.

Competition between ATP and glutamine for GS is likely to be relevant for the *in vivo* situation by adjusting the equilibrium between the A- and Q-state of GS. In the competitive titration experiments with glutamine in presence of ATP, biphasic curves were obtained with a maximum point at an ATP:Gln ratio of about 10:1 (Fig. 4 C). At this point, maximal binding of glutamine to GS at a single injection occurred. In the following injections, gradual saturation of the signal occurred. This glutamine: ATP ratio seems to be well tuned to the physiologically relevant concentrations of these metabolites. The intracellular concentration of glutamine may vary depending on the nitrogen source from 0.3 to 3 mM, whereas the cellular ATP level is considered to be maintained at concentrations in the low millimolar range (31). Remarkably, a recent study demonstrated unexpected heterogeneity of ATP concentrations in an *E. coli* cell population, ranging from 0.5 to 6.0 mM (35). It seems likely that at elevated concentrations of glutamine (corresponding to nitrogen excess conditions), GS is strongly impaired in ATP binding and is predominantly present in the Q-state. Under these conditions,

interaction of GS with TnrA is maximal. In accord, ATP was not able to quench the interaction between GS and TnrA in presence of 1 mM glutamine (see e.g. Figs. 3 A, 6 C). Conversely, at low cellular glutamine levels (nitrogen-limiting conditions), the A- and Q-states of GS are balanced. This explains why in cells grown under nitrogen-limited conditions, there is still some residual GS-TnrA interaction (Fig. 2 A). This residual interaction also explains the two times higher TnrA activity in a GS mutant strain in nitrogen limited cells (Fig. 1). Furthermore, the *in vitro* data indicate that the balance between A- and Q-state is slightly affected by the glutamate concentration (Fig. 8 E), due to competition with glutamine for the same binding site. Considering all these parameters, it appears that a small shift at the lower end of the intracellular glutamine concentrations (between 0.2 and 0.5 mM) could drastically change the ratio between A- and Q-state of GS and thus regulate the activity of the enzyme and its interaction with transcription factor TnrA in response to the nitrogen availability.

In addition to the ratio of glutamine, glutamate and ATP, the interaction between TnrA and GS is highly sensitive to AMP (Fig. 8 D, F), AMP itself did not stimulate the GS-TnrA complex formation on the DNA as strong as glutamine (Fig. 7 A), however successfully prevented the negative effect of 1 mM ATP (Fig. 8 D). AMP stimulated binding of GS to the TnrA-DNA complex more strongly when both glutamate and ATP were present (Fig. 8 F). Together, the balance between A and Q-state depends on the ratio between ATP, AMP, glutamine and glutamate. The amount of glutamate, which is an abundant compound in the cell, is maintained at a constantly high level (12,31). The ATP concentration varies in the millimolar range (31) and AMP and glutamine levels are prone to strong nutritional-dependent fluctuations. Therefore, the balance between A- and Q state of GS signals the relative concentration of these decisive effector molecules in a very sensitive manner.

The present SPR data on GS-TnrA interaction in the presence of DNA requires reconsideration of the mechanism how GS regulates the activity of the TnrA transcription factor. Previously, complex formation with GS was considered as a mechanism to prevent TnrA binding to DNA (9). This conclusion was based on EMSA assays, which only resolve highly stable complexes that are maintained during

electrophoresis (36). Here we used SPR, which monitors the formation and dissociation of the complex in real time (36). The SPR study clearly revealed that GS-complexed TnrA can still bind to the *nrgAB* promoter, even in the presence of excess glutamine. In contrast, GS diminished TnrA-DNA interaction on the *glnRA* promoter, probably due to a lower affinity of TnrA to this fragment. When TnrA was pre-loaded on the *nrgAB* promoter fragment, GS in the Q-state could easily bind to the TnrA-DNA complex. Since GS is a huge dodecameric molecule, which is 600 kDa in size, the binding of this large oligomeric machine to TnrA on the DNA should impair transcription. The formation of the TnrA-GS complex on the DNA probably results in the inactivation of the transcriptional activity of TnrA, as the large GS complex will sterically shield it from RNA-polymerase. Our refined model of TnrA control by GS thus assumes that under nitrogen excess conditions, where GS is mainly in the Q-state, it forms a complex with TnrA on positively regulated promoters and sterically blocks transcriptional activation. However, the negatively regulated promoter *glnRA* is liberated from TnrA and can now efficiently bind the GlnR-GS complex.

Taken together, our results suggest that *B. subtilis* GS can integrate the energy status (AMP:ATP ratio) and the nitrogen availability (using glutamine as nitrogen status reporter) of the cell, thereby modifying the transcriptional outcome through interaction with the central regulator of nitrogen metabolism TnrA. These sensory properties of GS have striking analogies to the signaling properties of the trimeric PII signal transduction proteins (37-39). In contrast, the *B. subtilis* PII protein GlnK appears to have acquired more specialized functions. Unlike other bacterial PII proteins, *B. subtilis* GlnK only interacts with ATP and lacks a clear 2-oxoglutarate response (8,17). The physiological role of the GlnK-TnrA complex formation might be a mechanism to protect TnrA from proteolytic degradation (17) and/or preserve GS biosynthetic activity from inhibitory interactions with TnrA (22). However, it plays only a minor role in the control of TnrA activity. Conversely, in *B. subtilis*, GS might have taken over the role of PII proteins as central integrator of the nitrogen- and energy status of the cells. Whether this is a specialized adaptation of *B. subtilis* or a general trait of Firmicutes bacteria requires further investigation.

Acknowledgments

Prof. Jörg Stülke and Dr. Fabian M. Commichau (Göttingen University) are gratefully acknowledged for providing *Bacillus subtilis* strains and plasmids. This research was supported by DFG Grant Fo195/9-2, DAAD Grant, Russian-German program ‘Michail Lomonosov’ A/12/75478, A/12/25777, 91583699, research fellowship of DAAD for PhD students and young scientists (50015537), RFBR grant 15-04-02583a

Conflict of interest

The authors declare no conflicts of interest.

Author contributions

KH performed the SPR assays and size exclusion analysis. AK performed ITC experiments, *in vivo* experiments and SPINE analysis. FG performed multi-angle light scattering analysis. KF conceived and coordinated the study and interpreted the results. All authors analyzed the results, wrote the manuscript and approved the final version of the manuscript.

REFERENCES

1. Wray, L. V., Jr., Ferson, A. E., Rohrer, K., and Fisher, S. H. (1996) TnrA, a transcription factor required for global nitrogen regulation in *Bacillus subtilis*. *Proc Natl Acad Sci U S A* **93**, 8841-8845
2. Fisher, S. H. (1999) Regulation of nitrogen metabolism in *Bacillus subtilis*: vive la difference! *Mol Microbiol* **32**, 223-232
3. Detsch, C., and Stulke, J. (2003) Ammonium utilization in *Bacillus subtilis*: transport and regulatory functions of NrgA and NrgB. *Microbiology* **149**, 3289-3297
4. Nakano, M. M., Hoffmann, T., Zhu, Y., and Jahn, D. (1998) Nitrogen and oxygen regulation of *Bacillus subtilis nasDEF* encoding NADH-dependent nitrite reductase by TnrA and ResDE. *J Bacteriol* **180**, 5344-5350
5. Wray, L. V., Jr., Zalieckas, J. M., and Fisher, S. H. (2000) Purification and *in vitro* activities of the *Bacillus subtilis* TnrA transcription factor. *J Mol Biol* **300**, 29-40
6. Yoshida, K., Yamaguchi, H., Kinehara, M., Ohki, Y. H., Nakaura, Y., and Fujita, Y. (2003) Identification of additional TnrA-regulated genes of *Bacillus subtilis* associated with a TnrA box. *Mol Microbiol* **49**, 157-165
7. Mirouze, N., Bidnenko, E., Noirot, P., and Auger, S. (2015) Genome-wide mapping of TnrA-binding sites provides new insights into the TnrA regulon in *Bacillus subtilis*. *Microbiologyopen* **4**, 423-435
8. Heinrich, A., Woyda, K., Brauburger, K., Meiss, G., Detsch, C., Stulke, J., and Forchhammer, K. (2006) Interaction of the membrane-bound GlnK-AmtB complex with the master regulator of nitrogen metabolism TnrA in *Bacillus subtilis*. *J Biol Chem* **281**, 34909-34917
9. Wray, L. V., Jr., Zalieckas, J. M., and Fisher, S. H. (2001) *Bacillus subtilis* glutamine synthetase controls gene expression through a protein-protein interaction with transcription factor TnrA. *Cell* **107**, 427-435
10. Fisher, S. H., and Wray, L. V., Jr. (2008) *Bacillus subtilis* glutamine synthetase regulates its own synthesis by acting as a chaperone to stabilize GlnR-DNA complexes. *Proc Natl Acad Sci U S A* **105**, 1014-1019
11. Commichau, F. M., Gunka, K., Landmann, J. J., and Stulke, J. (2008) Glutamate metabolism in *Bacillus subtilis*: gene expression and enzyme activities evolved to avoid futile cycles and to allow rapid responses to perturbations of the system. *J Bacteriol* **190**, 3557-3564
12. Gunka, K., and Commichau, F. M. (2012) Control of glutamate homeostasis in *Bacillus subtilis*: a complex interplay between ammonium assimilation, glutamate biosynthesis and degradation. *Mol Microbiol* **85**, 213-224
13. Brown, S. W., and Sonenshein, A. L. (1996) Autogenous regulation of the *Bacillus subtilis glnRA* operon. *J Bacteriol* **178**, 2450-2454
14. Schumacher, M. A., Chinnam, N. B., Cuthbert, B., Tonthat, N. K., and Whitfill, T. (2015) Structures of regulatory machinery reveal novel molecular mechanisms controlling *B. subtilis* nitrogen homeostasis. *Genes Dev* **29**, 451-464
15. Wray, L. V., Jr., and Fisher, S. H. (2007) Functional analysis of the carboxy-terminal region of *Bacillus subtilis* TnrA, a MerR family protein. *J Bacteriol* **189**, 20-27
16. Wray, L. V., Jr., and Fisher, S. H. (2008) *Bacillus subtilis* GlnR contains an autoinhibitory C-terminal domain required for the interaction with glutamine synthetase. *Mol Microbiol* **68**, 277-285
17. Kayumov, A., Heinrich, A., Fedorova, K., Ilinskaya, O., and Forchhammer, K. (2011) Interaction of the general transcription factor TnrA with the PII-like protein GlnK and glutamine synthetase in *Bacillus subtilis*. *FEBS J* **278**, 1779-1789
18. Meek, T. D., and Villafranca, J. J. (1980) Kinetic mechanism of *Escherichia coli* glutamine synthetase. *Biochemistry* **19**, 5513-5519
19. Wedler, F. C., and Horn, B. R. (1976) Catalytic mechanisms of glutamine synthetase enzymes. Studies with analogs of possible intermediates and transition states. *J Biol Chem* **251**, 7530-7538
20. Murray, D. S., Chinnam, N., Tonthat, N. K., Whitfill, T., Wray, L. V., Jr., Fisher, S. H., and Schumacher, M. A. (2013) Structures of the *Bacillus subtilis* glutamine synthetase dodecamer

- reveal large intersubunit catalytic conformational changes linked to a unique feedback inhibition mechanism. *J Biol Chem* **288**, 35801-35811
21. Deuel, T. F., and Prusiner, S. (1974) Regulation of glutamine synthetase from *Bacillus subtilis* by divalent cations, feedback inhibitors, and L-glutamine. *J Biol Chem* **249**, 257-264
 22. Fedorova, K., Kayumov, A., Woyda, K., Ilinskaja, O., and Forchhammer, K. (2013) Transcription factor TnrA inhibits the biosynthetic activity of glutamine synthetase in *Bacillus subtilis*. *FEBS Lett* **587**, 1293-1298
 23. Herzberg, C., Weidinger, L. A., Dorrbecker, B., Hubner, S., Stulke, J., and Commichau, F. M. (2007) SPINE: a method for the rapid detection and analysis of protein-protein interactions *in vivo*. *Proteomics* **7**, 4032-4035
 24. Gibson, D. G., Young, L., Chuang, R. Y., Venter, J. C., Hutchison, C. A., 3rd, and Smith, H. O. (2009) Enzymatic assembly of DNA molecules up to several hundred kilobases. *Nat Methods* **6**, 343-345
 25. Saxild, H. H., and Nygaard, P. (1987) Genetic and physiological characterization of *Bacillus subtilis* mutants resistant to purine analogs. *J Bacteriol* **169**, 2977-2983
 26. Hart, D. J., Speight, R. E., Cooper, M. A., Sutherland, J. D., and Blackburn, J. M. (1999) The salt dependence of DNA recognition by NF-kappaB p50: a detailed kinetic analysis of the effects on affinity and specificity. *Nucleic Acids Res* **27**, 1063-1069
 27. Stevenson, C. E., Assaad, A., Chandra, G., Le, T. B., Greive, S. J., Bibb, M. J., and Lawson, D. M. (2013) Investigation of DNA sequence recognition by a streptomycete MarR family transcriptional regulator through surface plasmon resonance and X-ray crystallography. *Nucleic Acids Res* **41**, 7009-7022
 28. Liaw, S. H., and Eisenberg, D. (1994) Structural model for the reaction mechanism of glutamine synthetase, based on five crystal structures of enzyme-substrate complexes. *Biochemistry* **33**, 675-681
 29. Krajewski, W. W., Jones, T. A., and Mowbray, S. L. (2005) Structure of *Mycobacterium tuberculosis* glutamine synthetase in complex with a transition-state mimic provides functional insights. *Proc Natl Acad Sci U S A* **102**, 10499-10504
 30. Wray, L. V., Jr., and Fisher, S. H. (2010) Functional roles of the conserved Glu304 loop of *Bacillus subtilis* glutamine synthetase. *J Bacteriol* **192**, 5018-5025
 31. Bennett, B. D., Kimball, E. H., Gao, M., Osterhout, R., Van Dien, S. J., and Rabinowitz, J. D. (2009) Absolute metabolite concentrations and implied enzyme active site occupancy in *Escherichia coli*. *Nat Chem Biol* **5**, 593-599
 32. Ikeda, T. P., Shauger, A. E., and Kustu, S. (1996) *Salmonella typhimurium* apparently perceives external nitrogen limitation as internal glutamine limitation. *J Mol Biol* **259**, 589-607
 33. Almassy, R. J., Janson, C. A., Hamlin, R., Xuong, N. H., and Eisenberg, D. (1986) Novel subunit-subunit interactions in the structure of glutamine synthetase. *Nature* **323**, 304-309
 34. Eisenberg, D., Gill, H. S., Pfluegl, G. M., and Rotstein, S. H. (2000) Structure-function relationships of glutamine synthetases. *Biochim Biophys Acta* **1477**, 122-145
 35. Yaginuma, H., Kawai, S., Tabata, K. V., Tomiyama, K., Kakizuka, A., Komatsuzaki, T., Noji, H., and Imamura, H. (2014) Diversity in ATP concentrations in a single bacterial cell population revealed by quantitative single-cell imaging. *Sci Rep* **4**, 6522
 36. Matos, R. G., Barbas, A., and Arraiano, C. M. (2010) Comparison of EMSA and SPR for the characterization of RNA-RNase II complexes. *Protein J* **29**, 394-397
 37. Forchhammer, K. (2008) P(II) signal transducers: novel functional and structural insights. *Trends Microbiol* **16**, 65-72
 38. Huergo, L. F., Chandra, G., and Merrick, M. (2013) PII signal transduction proteins: nitrogen regulation and beyond. *FEMS Microbiology Reviews* **37**, 251-283
 39. Forchhammer, K., and Luddecke, J. (2015) Sensory properties of the P signalling protein family. *FEBS J*

40. Blencke, H. M., Reif, I., Commichau, F. M., Detsch, C., Wacker, I., Ludwig, H., and Stulke, J. (2006) Regulation of citB expression in *Bacillus subtilis*: integration of multiple metabolic signals in the citrate pool and by the general nitrogen regulatory system. *Arch Microbiol* **185**, 136-146
41. Martin-Verstraete, I., Debarbouille, M., Klier, A., and Rapoport, G. (1994) Interactions of wild-type and truncated LevR of *Bacillus subtilis* with the upstream activating sequence of the levanase operon. *J Mol Biol* **241**, 178-192
42. Stragier, P., Bonamy, C., and Karmazyncampelli, C. (1988) Processing of a Sporulation Sigma Factor in *Bacillus-Subtilis* - How Morphological Structure Could Control Gene-Expression. *Cell* **52**, 697-704

The abbreviations used are: GS, glutamine synthetase; SPR, Surface Plasmon Resonance; ITC, Isothermal Titration Calorimetry, SPINE, Strep-protein interaction experiment, PFA, paraformaldehyde, MSX, methionine sulfoximine, AMP-PNP, adenosine 5'-(β,γ -imido)triphosphate, ATP γ S, adenosine 5'-(γ -thio)triphosphate tetralithium salt.

FIGURE LEGENDS

FIGURE 1. Expression of a β -galactosidase reporter under control of the TnrA-dependent *nrgA* promoter reveals transcriptional activity of TnrA. *B. subtilis* cells were grown under nitrogen-limited conditions either using 1.5 mM glutamine (circles) or 20 mM nitrate (squares) for strain GP250 (wild type background), and using 1.5 mM glutamine (triangles) for strain GP251 (*glnA*⁻ background).

FIGURE 2. SPINE analysis of TnrA interacting with GlnK and GS under limiting (1.5 mM glutamine) or sufficient (15 mM glutamine) nitrogen conditions. *B. subtilis* *tnrA*⁻, *glnK*⁻ and *glnA*⁻ mutants producing respectively strepII-tagged recombinant TnrA-ST, GlnK-ST and GS-ST were grown in SMM medium supplemented with 1.5 mM glutamine and shifted to 15 mM glutamine as indicated. After treating the cells with 0.6% PFA, TnrA-ST (A), GlnK-ST and GS-ST (B) were purified from crude extracts on strep-tactin sepharose; the elution fractions were analyzed by immunoblotting using anti-TnrA, anti-GlnK and anti-GS antibodies.

FIGURE 3. SPR analysis of GS TnrA interplay. GS was loaded on the TnrA chip surface either without effector molecules (continuous line) or in the presence of 1mM ATP (dotted line), 1 mM glutamine (A) or 1 mM MSX (B) (dashed line), 1 mM ATP and 1 mM glutamine (A) /1 mM MSX (B) (thin dashed line).

FIGURE 4. Analysis of ligand binding properties of GS by ITC. Glutamine, ATP or AMP in concentrations as indicated were injected (45 times 6 μ l) into 20 μ M (A, B) or 10 μ M (C – F) GS with stirring of 155 rpm. (A) Titration with 2 mM glutamine. Six (5.6 ± 0.16) binding sites were predicted from the titration data. (B) Titration with 2 mM ATP. Six (5.5 ± 0.13) binding sites were predicted. (C) Titration of GS in presence of 2 mM ATP with 2 mM glutamine. The glutamine concentration at the maximum enthalpy (highest point of the curve) 173 ± 34.7 μ M. (D) Titration of GS in presence of 0.5 mM glutamine with 5 mM ATP. The ATP concentration at the maximum enthalpy (lowest point of the curve) 421 ± 31.2 μ M. (E) Titration of GS in presence of 2 mM ATP with 2 mM AMP. The AMP concentration at the maximum enthalpy (highest point of the curve) 186 ± 14.2 μ M. (F) Titration of GS in presence of 0.5 mM AMP with 5 mM ATP. The ATP concentration at the maximum enthalpy (lowest point of the curve) 23 ± 4.2 μ M.

FIGURE 5. The pattern of alternating positive (synergistic) and negative (antagonistic) cooperative interactions between the sequential glutamine (dashed line) and ATP (continuous line) binding sites of GS. K_D values were obtained by fitting ITC data using a binding model of six sequential binding sites.

FIGURE 6. SPR analysis of TnrA binding with 30-mer *nrgAB* or 54-mer *glnRA* promoter fragment. (A) TnrA was injected onto immobilized DNA surface (thin continuous line for the *nrgAB* promoter, thin dashed line for the *glnRA* promoter) alone or in the mixture with GS in the 3 to 1 ratio (continuous line for the *nrgAB* promoter, dashed line for the *glnRA* promoter). (B) TnrA was injected onto immobilized *nrgAB* promoter fragment (continuous line) or *glnRA* promoter fragment (dashed line) and then GS was loaded on the TnrA-DNA chip surface. (C) TnrA was injected onto immobilized *nrgAB* promoter fragment subsequently GS was injected onto immobilized TnrA-DNA surface without effector molecules (continuous line), in presence of 1 mM glutamine (dashed line) or 1 mM ATP (dotted line) and in presence of 1 mM ATP and 1 mM glutamine (thin dashed line). (D) TnrA was injected onto immobilized *nrgAB* promoter fragment subsequently GS was injected without effector molecules (continuous line) in presence of 1 mM methionine sulfoximine (MSX) (dashed line) or 1 mM ATP (dotted line), in presence of 1 mM ATP and 1 mM glutamine.

FIGURE 7. SPR analysis of GS binding to TnrA immobilized on the 30-mer *nrgAB* promoter fragment in presence of different effector molecules. (A) GS was loaded on the TnrA-DNA chip surface without effector molecules or in presence of 1 mM MSX, 1 mM ATP, 1 mM ATP and 1 mM MSX, 1 mM ADP, 1 mM ADP and 1 mM MSX, 1 mM AMP, 1 mM AMP and 1 mM MSX as indicated. (B) GS was loaded on the TnrA-DNA chip surface without effector molecules. or in presence of 1 mM MSX, 1 mM AMP-PNP, 1 mM AMP-PNP and 1 mM MSX, 1 mM ATP- γ -S (dotted line), 1 mM ATP- γ -S and 1 mM MSX as indicated.

FIGURE 8. Influence of glutamine or AMP on GS interaction with TnrA immobilized on the 30-mer *nrgAB* promoter fragment. GS in the presence or absence of various effector molecules was injected on surface immobilized TnrA-DNA complex. The increase in resonance units (RU) relative to a control injection with GS in the absence of the variable effector molecule was recorded (normalized Δ RU) Glutamine was used as variable effector molecule in (A), (C) and (E), and AMP was used as variable effector molecule in (B) (D) and (F). No additional effector molecules were present in (A) and (B). ATP at a constant concentration of 1 mM was present in (C) and (D), and constant concentration of 1 mM ATP and 10 mM glutamate was present in (E) and (F). The obtained values were fitted to the equation “one site - specific binding with Hill slope” using GraphPad Prism.

FIGURE 9. Size exclusion chromatography of cross-linked GS, TnrA and GS-TnrA complexes. (A) The elution profiles of GS (V_e =1.14 ml, 1.45 ml, 1.59 ml), TnrA (V_e =1.66 ml), a mixture containing GS and TnrA (1 dodecamer : 6 dimers) in presence of 1 mM MSX (V_e =1.12ml, 1.45 ml, 1.59 ml) or in presence of 1 mM MSX and 1 mM ATP (1.14 ml, 1.45 ml, 1.59 ml) are shown. (B) The elution profiles of GS (V_e =1.11 ml, 1.43 ml, 1.58 ml), TnrA (V_e =1.64 ml) and a mixture of GS and TnrA (1 dodecamer : 6 dimers) in presence of 1 mM glutamine (V_e =1.12ml, 1.45 ml, 1.59 ml). The elution peak at 0.9 ml most likely corresponds to protein aggregates. (C) SEC-MALS profiles for GS and the GS:TnrA complex. Both preparations were separated by size exclusion chromatography and the measured molar masses are shown as dotted (GS-TnrA complex) or dotted and dashed lines (GS) underneath the peak fractions.

Table 1. Strains and plasmids used in this study

Strains and plasmid	Genotype	Source/Reference ^a
<i>B. subtilis</i> 168	<i>trpC2</i>	Laboratory strain collection
<i>B. subtilis</i> GP250	<i>trpC2 amyE::(nrgA-lacZ aphA3)</i>	(3)
<i>B. subtilis</i> GP251	<i>trpC2 amyE::(nrgA-lacZ aphA3) ΔglnA::cat</i>	pGP176 → GP250
<i>B. subtilis</i> GP253	<i>trpC2 amyE::(nrgA-lacZ aphA3) ΔglnK::cat</i>	(3)
<i>B. subtilis</i> GP259	<i>trpC2 ΔglnK::cat</i>	GP253 → 168
<i>B. subtilis</i> GP252	<i>trpC2 amyE::(nrgA-lacZ aphA3) ΔtnrA</i>	(40)
Plasmids	Purpose	Source/Reference
pBQ200	Expression vector for <i>B. subtilis</i>	(41)
pDG148	Expression vector	(42)
pET15b TnrA	Overexpression of His-tagged TnrA in <i>E. coli</i>	(8)
pET15b GlnR	Overexpression of His-tagged GlnR in <i>E. coli</i>	(22)
pET15b GS	Overexpression of His-tagged GS in <i>E. coli</i>	This study
pDG-GlnK-ST	Overexpression of StrepII-tagged GlnK in <i>E. coli</i> and <i>B. subtilis</i>	(8)
pDG-TnrA-ST	Overexpression of StrepII-tagged TnrA in <i>E. coli</i> and <i>B. subtilis</i>	This study
pGP-pTnrA-ST	Expression of StrepII-tagged TnrA in <i>B. subtilis</i> from <i>tnrA</i> promoter, Em	This study
pGP174	Overexpression of StrepII-tagged GS in <i>E. coli</i>	(8)
pGP176	Inactivation of the <i>B. subtilis glnA</i> gene	(3)
pGP177	Overexpression of N-terminally StrepII-tagged GS in <i>B. subtilis</i>	This study
pGP380	Overexpression of N-terminally StrepII-tagged proteins in <i>B. subtilis</i>	(23)

^aArrows indicate construction by transformation.

Table 2. Sequences of oligonucleotides used for SPR spectroscopy

Oligonucleotide designation ^a	Length (bases)	Sequence 5' to 3'
<i>PnrgAB</i> _30mer_F	30	AAAACCATGTCAGGAAATCTTACATGAAAA
<i>PnrgAB</i> _30mer_R	50	TTTTCATGTAAGATTTCTGACATGGTTTTCTACCCTACGTCCTCCTGC
<i>PglnRA</i> _54mer_F	54	GATTTGATGTTAAGAATCCTTACATCGTATTGACACATAATATAACATCACCTA
<i>PglnRA</i> _54mer_R	74	TAGGTGATGTTATATTATGTGTCAATACGATGTAAGGATTCTTAACATCAAATCCTACCCTACGTCCTCCTGC
Unspecific DNA_30mer_F	30	CAGTGAGGCACCTATCTCAGCGATCTGTCT
Unspecific DNA_30mer_R	50	AGACAGATCGCTGAGATAGGTGCCTCACTGCCTACCCTACGTCCTCCTGC
Unspecific DNA_54mer_F	54	CAGTGAGGCACCTATCTCAGCGATCTGTCTCAGTGAGGCATCTCAGCGATCTGT
Unspecific DNA_54mer_R	74	ACAGATCGCTGAGATGCCTCACTGAGACAGATCGCTGAGATAGGTGCCTCACTGCCTACCCTACGTCCTCCTGC

^a *F* = forward strand; *R* = reverse strand

Table 3. Analysis of GS:TnrA stoichiometry by SPR spectroscopy. His-tagged GS was immobilized on a sensor chip and StrepII-tagged TnrA was used as analyte at various concentrations. The stoichiometry was calculated as described in the experimental procedures.

GS captured (RU)	TnrA (μ M)	measured Δ RU	stoichiometry
5172	1	562	2.3 (no saturation)
5873	2	916	3.3
5849	4	935	3.4
6161	8	950	3.3

Figure 1

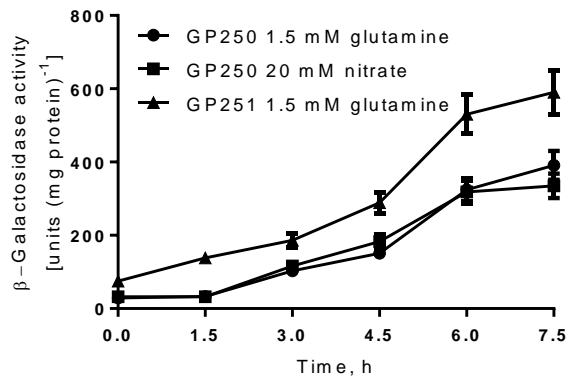


Figure 2

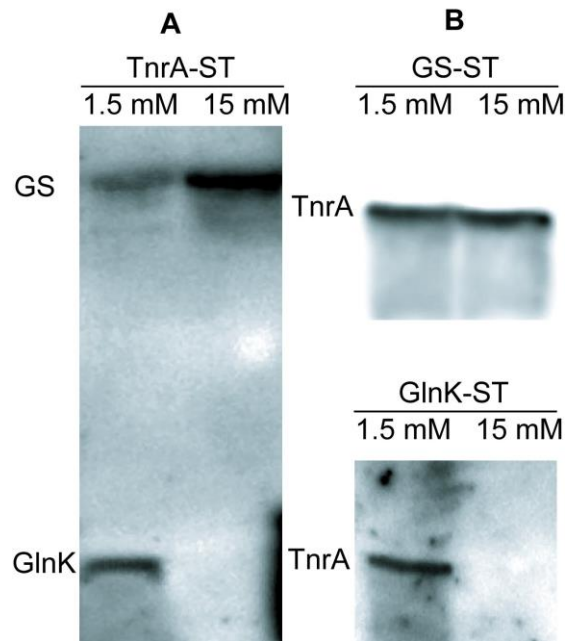


Figure 3

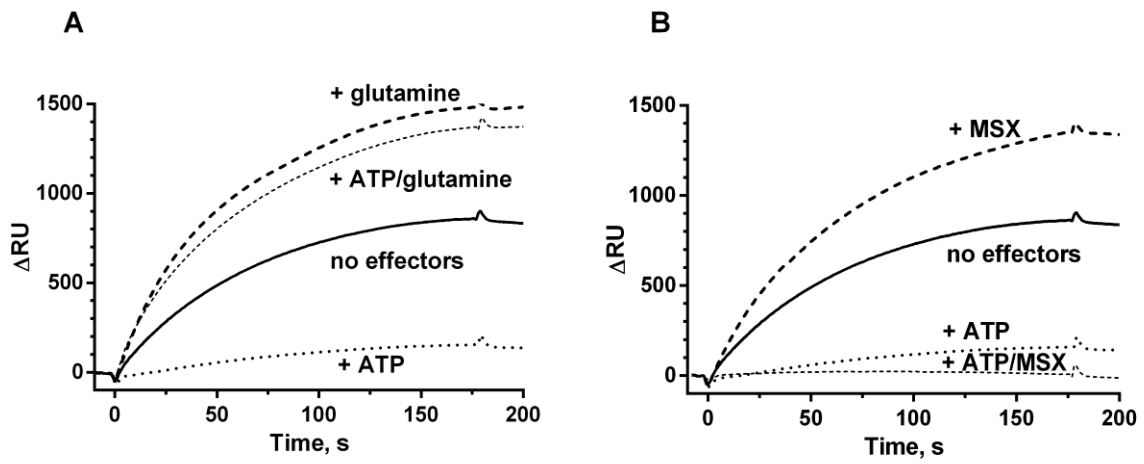


Figure 4

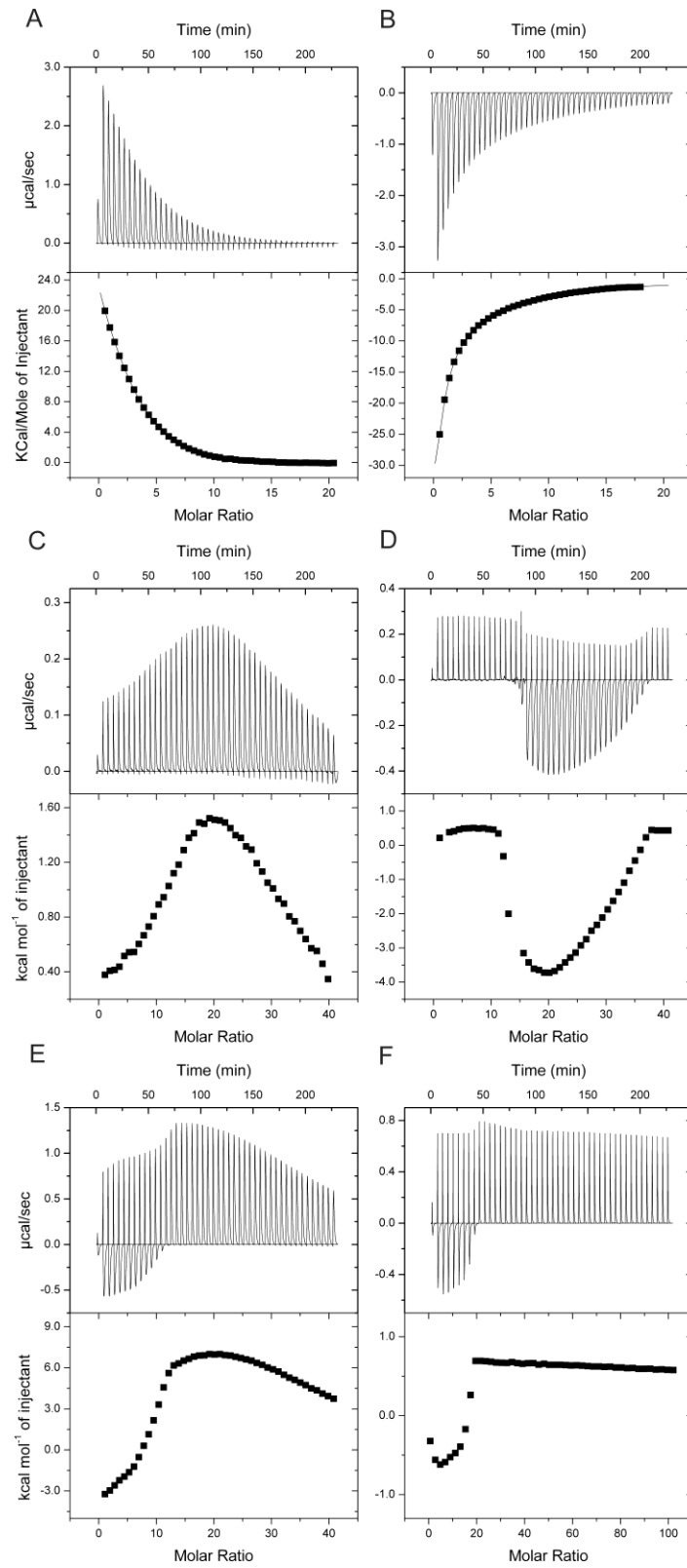


Figure 5

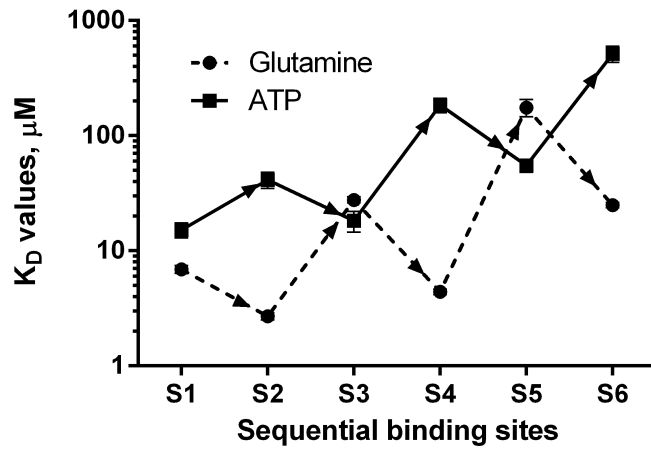


Figure 6

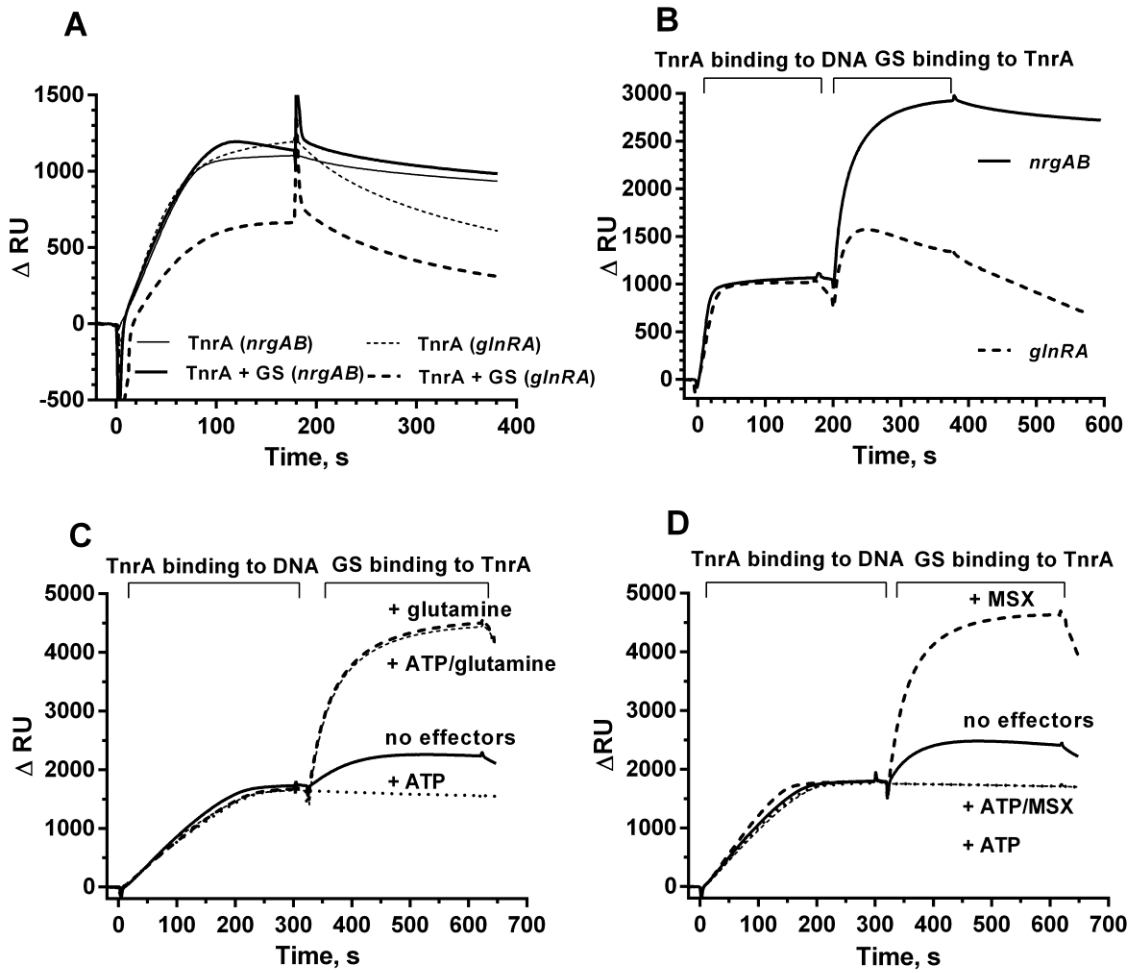


Figure 7

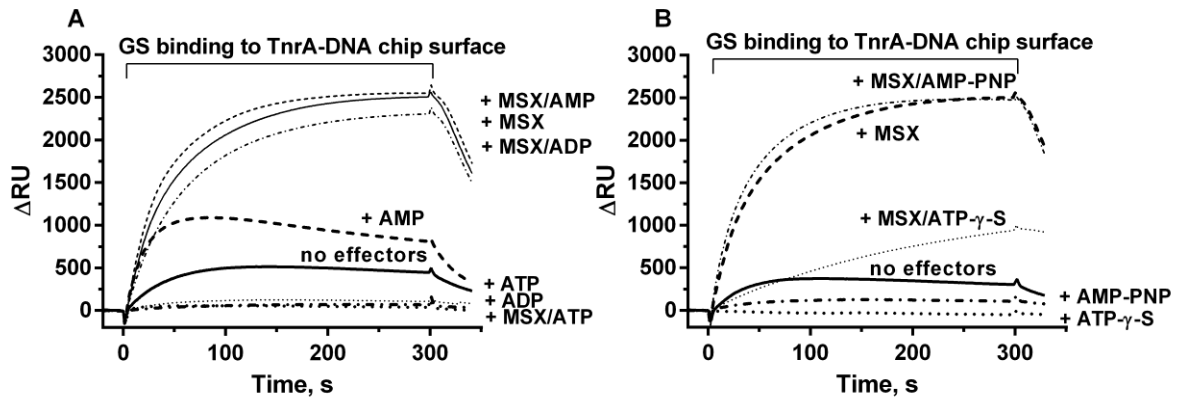


Figure 8

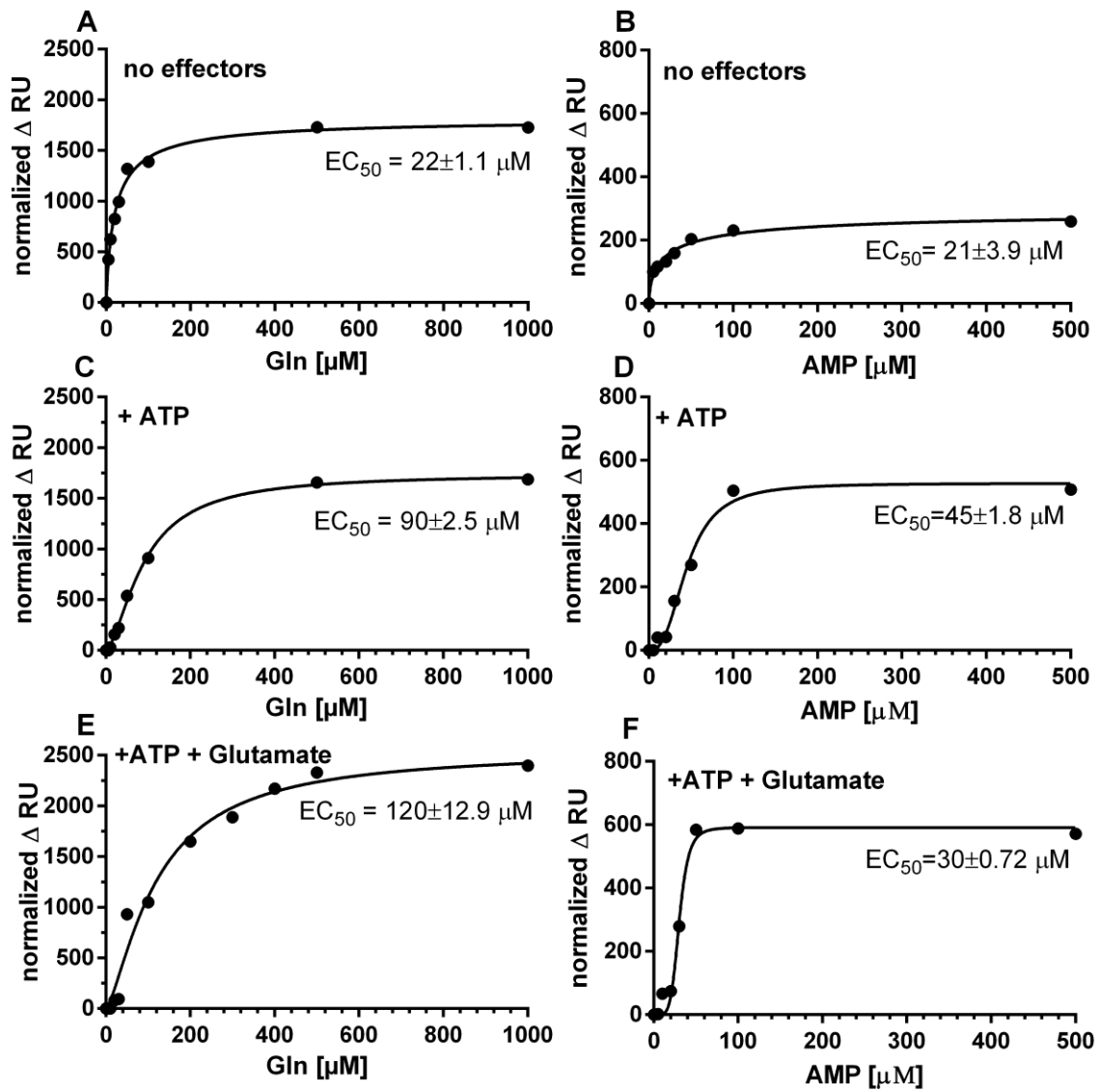
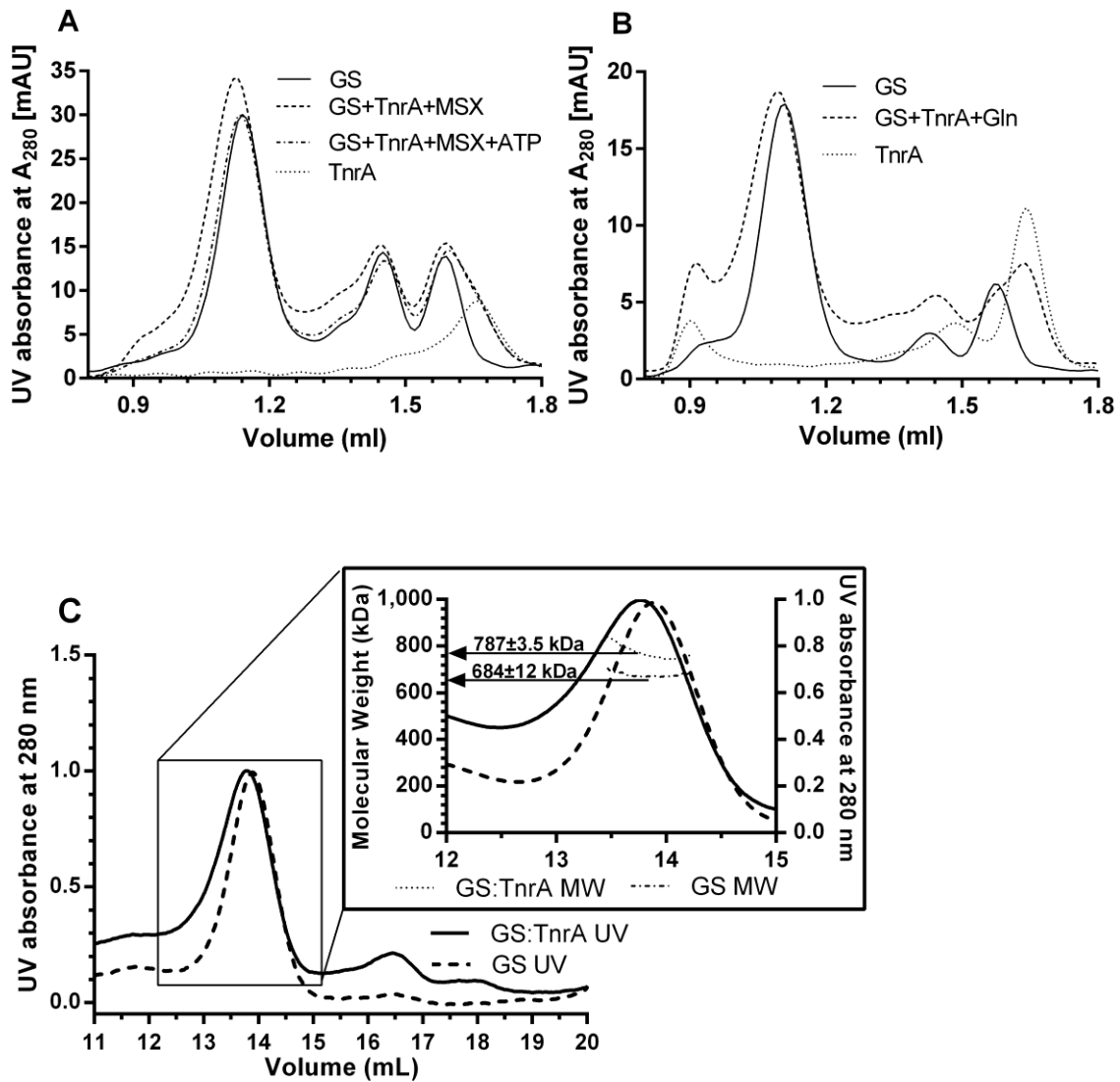
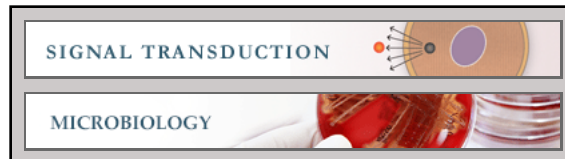


Figure 9



Signal Transduction:
**The molecular basis of TnrA control by
glutamine synthetase in *Bacillus subtilis***

Ksenia Hauf, Airat Kayumov, Felix Gloge and
Karl Forchhammer
J. Biol. Chem. published online December 3, 2015



Access the most updated version of this article at doi: [10.1074/jbc.M115.680991](https://doi.org/10.1074/jbc.M115.680991)

Find articles, minireviews, Reflections and Classics on similar topics on the [JBC Affinity Sites](#).

Alerts:

- [When this article is cited](#)
- [When a correction for this article is posted](#)

[Click here](#) to choose from all of JBC's e-mail alerts

This article cites 0 references, 0 of which can be accessed free at
<http://www.jbc.org/content/early/2015/12/03/jbc.M115.680991.full.html#ref-list-1>